Journal of Energy
VOLUME 75 Number 1 | 2026
journal homepage: http://journalofenergy.com/

Hybrid Shielding Calculations of GBC32 Cask

Mario Matijević, Matej Pekeč

Summary **— This paper presents an evaluation of the shielding performance of the Generic Burnup Credit Cask (GBC-32) containing 32 Westinghouse 17x17 spent fuel assemblies. The spent fuel source term characterization was done in previous work, for which burnup/depletion calculations of TRITON-NEWT in tandem with ORIGEN-S were performed, generating collapsed cross section libraries as a function of fuel enrichment and burnup level. The hybrid shielding methodology of MAVRIC sequence in SCALE6.1.3 code was used to quantify neutron-gamma radiation field and dose rates around the cask, taking previously prepared source terms with ORIGEN-ARP module. For that purpose, to expedite the input preparation, a special routine in C-language was programmed to read ORIGEN-ARP multigroup output data and provide normalized neutron-gamma (n-g) spectra with the associated intensities (particles/s/MTU). This distributed multisource in Monte Carlo cask model included spent fuel neutrons and photons, photons from (n,g) reactions and photons from activated upper/lower hardware regions of spent fuel assemblies. Different fuel loading patterns were investigated, ranging from generic (one zone) to more realistic one (three zones) using averaged values of burnup, fuel enrichment and cooling time period. The FW-CADIS variance reduction technique was successfully applied for achieving global neutron-gamma flux convergence in radial and axial directions of the cask. The presented MC dosimetry results correspond to normal cask conditions, but an accidental scenario was also investigated, for which the resin neutron shield was removed from the shielding configuration.**

Keywords **— SCALE6.1.3, FW-CADIS, cask, shielding, dose rates**

I. Introduction

The GBC-32 cask is an artificial model that combines the information from several actual cask submittals in the shielding safety analysis report (SARP). It was developed for the purpose of burnup-credit criticality studies with all the attributes of a realistic storage or transportation cask [1]. The shielding study of the GBC-32 cask was performed in this paper to evaluate compliance with dose rate limits of 10CFR71.47 for normal conditions and 10CFR71.51 for accidental conditions [2]. These regulatory limits are 200 mrem/h on the cask top and bottom surface, and 10 mrem/h at the 2 m location away from the cask. For accidental conditions this regulatory limit is increased to 1000 mrem/h.

(Corresponding author: Mario Matijević)
Mario Matijević and Matej Pekeč are with the University of Zagreb Faculty of Electrical Engineering and Computing, Zagreb, Croatia (email: mario.matijevic@fer.hr, matej.pekec@fer.hr)

The cask body is basically consisting of inner shell (stainless steel) and outer shell (resin) with a top and bottom lid providing shielding in axial direction. To provide a conservative approach, the impact limiters (wood inside steel casing) and boral panels between fuel assemblies (FAs) were omitted from the model. The spent fuel source terms used in this study were previously prepared with ORIGEN-ARP module [3], based on calculation framework of the TRITON-NEWT in tandem with ORIGEN-S module [4], generating collapsed cross section libraries from 238 to 49 neutron groups as a function of fuel enrichment and burnup level [5]. The fuel assembly is optimized Westinghouse 17x17 (OFA), with specific dimensions and materials taken from the reference [1]. From the shielding perspective, one arrives at distributed multisource in Monte Carlo (MC) cask model, including spent fuel neutrons and photons, photons from (n,g) reactions and photons from activated upper/lower hardware regions of spent fuel assemblies. This model was investigated with several variance reduction (VR) techniques and satisfactory convergence of neutron and gamma (n-g) dose rates was obtained.

This paper is organized as follows. Chapter 2 provides information about the cask geometry and source data preparation. The SCALE6.1.3/MAVRIC hybrid shielding sequence, used for cask calculations, is presented in Chapter 3. The cask shielding results are given in Chapter 4, ranging from generic to detailed source description, and from analog MC simulation to an optimized one, using FW-CADIS methodology. The accidental neutron dose rates are also quantified and compared to normal dose rates. Lastly, the conclusions are given in Chapter 5, while the list of used references is provided at the end of the paper.

II. Cask source and geometry specification

The source terms of spent fuel assemblies cover two regions: the active fuel region (neutrons and gammas) and upper/lower hardware region (gammas) simulating presence of ^{60}Co originating from impurity ^{59}Co, which can be found in steel and Inconel structural materials. The ORIGEN-ARP code of SCALE6.1.3 code [4] was used to calculate multigroup n-g sources for active fuel region. A small C-program [6] was written which reads the ORIGEN output file and generates normalized n-g spectra with the associated n-g intensities (particles/s/MTU) as a function of time. The broad-group library "v7-27n19g" was used for ORIGEN calculations, matching format of the broad shielding library used by Monaco MC module [4]. The quantities of structural material in the top, plenum and bottom hardware regions of FA are taken from reference [2] and presented in Table 1. The curies of ^{60}Co per kg of steel were 10 Ci/kg (bottom nozzle), 2.5 Ci/kg (top nozzle) and 4.6 Ci/kg (plenum), so total curie loadings were 24.1 Ci (top endfitting + plenum) and 58.9 Ci (bottom endfittings).

Mario Matijević, Matej Pekeč, Hybrid Shielding Calculations of GBC32 Cask, Journal of Energy, vol. 75 Number 1 (2026), 3–8
https://doi.org/10.37798/2026751724

TABLE I.
FUEL ASSEMBLY HARDWARE PARTS AND MATERIALS

FA part	Weight (kg) / FA	Zone	Material
Bottom nozzle	5.897	bottom	Stainless steel 304
Hold-down spring	0.960	top	Inconel 718
Spacer – plenum	0.885	gas plenum	Inconel 718
Top nozzle	6.890	top	Stainless steel 304
Grid sleeve	0.091	gas plenum	Stainless steel 304

The generic cask source has only one fuel zone (32 fuel elements of OFA Westinghouse 17x17 type) with an averaged values of: enrichment e=4.0%, burnup BU=45.0 GWd/MTU, cooling time=10 years, specific power=40.0 MW/MTU, and uranium weight of 0.4634 MTU per FA [5]. The pellet density was 10.357 g/cm^3 with 94.5% theoretical value, and moderator density was 0.71 g/cm^3. The ORIGEN-ARP [3] was used to make burnup-depletion calculations (12 cases in total), using three cross section libraries per irradiation cycle and one library for a decay cycle. For a generic neutron case, one fuel zone with total of 7.718e+09 n/s was defined while a generic photon case had multiple gamma sources: one fuel zone with total of 1.136e+17 phot/s and three hardware regions (bottom nozzle, upper nozzle and plenum) giving additional 3x32 or 96 distributed ^{60}Co sources.

The more realistic cask source has 32 FAs in 3 different fuel zones, with zone-wise neutron/gamma spectra and particle intensities calculated by ORIGEN-ARP module:

- Zone 1 (red): 8 FA, BU=48 GWd/MTU, e=4.5%, cooling time = 14 years
- Zone 2 (blue): 12 FA, BU=40 GWd/MTU, e=3.6%, cooling time = 12 years
- Zone 3 (white): 12FA, BU=30 GWd/MTU, e=3.0%, cooling time=30 years

The specific thermal power was assumed to be 36.0 MW/MTU. This more realistic source description introduces an extra burden on source sampling routines during Monaco MC simula-tions, taking more CPU time. The comparison of a generic and realistic cask source is shown in Figure 1.

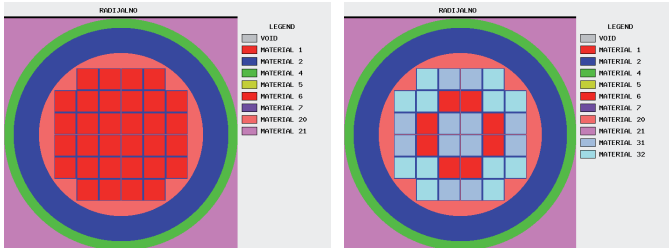

Fig. 1. Generic (left) and more realistic (right) cask source description

An important factor for radiation shielding characterization of the cask was inclusion of an axial normalized burnup profile, producing a biased sampling of source neutrons and photons along the active fuel length (Figure 2). This ultimately leads to a more realistic, asymmetrical dose distributions. This function in form of binned histogram was imported from the reference [1] and total of 18 fuel axial segments with corresponding probabilities were included in the MAVRIC cask model. The same burnup profile was used for sampling neutrons and photons, which is a reasonable approach.

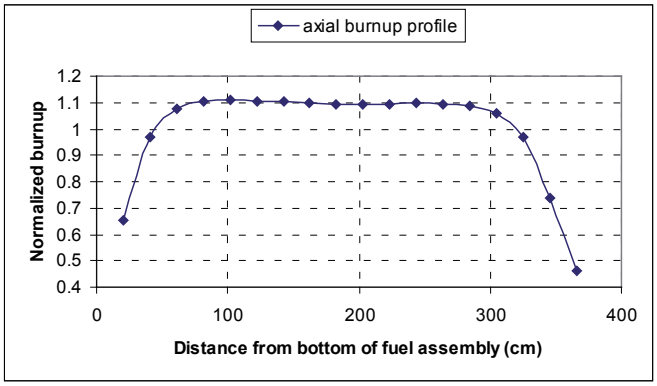

Fig. 2. Axial burnup profile of the spent fuel

The sources of fuel assemblies are thus spatially distributed, forming sources from the active fuel region and from the upper/lower hardware regions. These sources can be further broken into neutron and gamma-ray components, with separate intensities and spectrum. The active fuel region is a neutron-gamma emitter while the hardware region contains only gamma sources from activated ^{60}Co (steel impurity). The neutron-gamma sources in active FA region were calculated using ORIGEN-ARP code, using previously generated cross section libraries for OFA fuel [5]. Gamma sources for fuel assembly hardware parts were calculated using industry values i.e. the curies of cobalt per kg of specific steel part. Figure 3 shows MAVRIC model of the GBC-32 cask for a normal transport condition, while accidental case assumes removal of the resin (green layer) from the model. The truncated model on the right has a helium gas removed around FA cells for clarity. Also, this model corresponds to a realistic cask source with three FA zones. The FAs were homogenized by isotopic mass preservation and modelled as stacked axial layers. To be more precise, the fuel, cladding and hardware volume fractions were smeared over the FA basket. The cask body dimensions are taken from reference [2] and given in Table 2.

TABLE II.
CASK GLOBAL DIMENSIONS

Model section	Radius (cm)	Total height (cm)
Cavity (He gas)	87.5	425.76
Steel shell	114.5	495.76
Resin shell	124.5	376.00

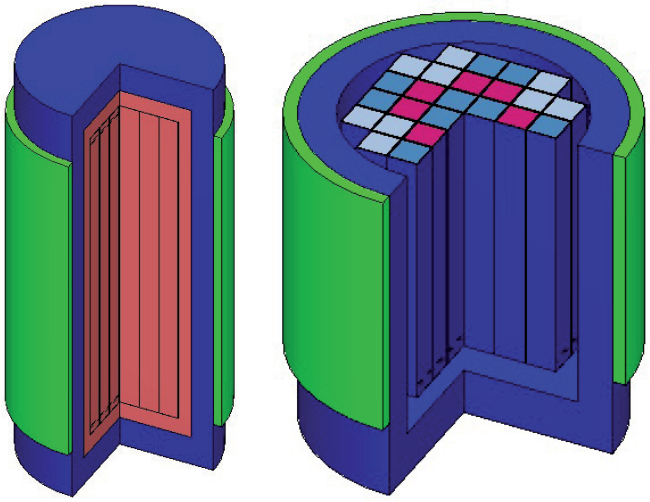

Fig. 3. MAVRIC model of the GBC-32 cask with a three FA zones

Mario Matijević, Matej Pekeč, Hybrid Shielding Calculations of GBC32 Cask, Journal of Energy, vol. 75 Number 1 (2026), 3–8
https://doi.org/10.37798/2026751724

III. SCALE6.1.3 SHIELDING COMPUTATIONAL TOOLS

The SCALE6.1.3 code's main shielding sequence is MAVRIC, based on the CADIS [7] and FW-CADIS [8] methods utilizing SN solver Denovo [9] for deterministic VR calculation and subsequent accelerated MC Monaco particle transport [4]. For both CADIS and FW-CADIS, the particle average weight is inversely related to an adjoint flux [10] value throughout phase-space, so locations of high importance (i.e. high adjoint flux) will have low-weighted particles and vice versa. This implies that adjoint source location for optimized MC results will represent spatial attractor for the source particles, giving »reasonable« MC results in-between regions. Depending on the volumetric size and placement of the adjoint source, it is possible to produce MC results with reasonable statistics even between the forward source and the adjoint source, but it is highly case-specific.

The detector response is found by integrating the product of the detector cross-section $\sigma_d(\vec{r},E)$ and flux over detector volume V_D:

$$R=\int_{V_D}\int_E \sigma_d(\vec{r},E)\phi(\vec{r},E)dVdE \tag{1}$$

Alternatively, if we approximate the adjoint scalar flux with a quick SN solution, where the adjoint source is set as $q^\dagger(\vec{r},E)=\sigma_d(\vec{r},E)$, then the detector response is found by integrating the product of the forward source $q(\vec{r},E)$ and the adjoint flux $\phi^\dagger(\vec{r},E)$ over the source volume V_S:

$$R=\int_{V_S}\int_E q(\vec{r},E)\phi^\dagger(\vec{r},E)dVdE\,. \tag{2}$$

The biased source distribution $\hat{q}(\vec{r},E)$ is thus based on an estimate of the adjoint scalar flux, from which the response R can be made using Eq. (2):

$$\hat{q}(\vec{r},E)=\frac{\phi^\dagger(\vec{r},E)q(\vec{r},E)}{R}=\frac{\phi^\dagger(\vec{r},E)q(\vec{r},E)}{\int_{V_S}\int_E q(\vec{r},E)\phi^\dagger(\vec{r},E)dVdE}, \tag{4}$$

where $\phi^\dagger(\vec{r},E)$, $q(\vec{r},E)$ and R are the scalar adjoint function, the source emission probability (forward source), and the total detector response, respectively [4]. For transport biasing the weight window technique is employed, that is, space-energy dependent geometric splitting/roulette. Biased source and weight-window lower bounds are consistent, so the source particles are created with statistical weights within weight windows:

$$\overline{w}(\vec{r},E)=\frac{q(\vec{r},E)}{\hat{q}(\vec{r},E)}=\frac{R}{\phi^\dagger(\vec{r},E)}=\frac{\int_{V_S}\int_E q(\vec{r},E)\phi^\dagger(\vec{r},E)dVdE}{\phi^\dagger(\vec{r},E)}. \tag{5}$$

The inverse relationship between particle statistical weight and adjoint function is crucial, implying more splitting of low-weighted particles in important regions of the MC model. The dose mapping of the cask involves calculation of near and far detector dose rates, so FW-CADIS methodology was selected for this problem. To expedite many simulation cases, Denovo SN solver [11] was used with "basic" FW-CADIS parameters: S4 quadrature set, P1 scattering cross section expansion (Legendre order), step characteristic (SC) spatial differencing, and diagonal transport correction. The macromaterial option mixed cca 10 pure materials into 3-4 times more pseudomaterials (case dependent) on uniform SN mesh with 768e3 cells covering global unit. Even a low-quality deterministic solution will be a good enough approximation for biasing the final MC simulation. The adjoint source was always defined as dry air external to the cask with spectrum corresponding to dose rate function (9029-neutrons or 9504-photons). Monaco MC was used with 5e6 histories and shielding library was "v7-27n19g" for both SN and MC portions of calculations [12]. The cylindrical mesh tally with 150e6 cells was used for capturing global n-g dose rates.

IV. GBC-32 CASK SHIELDING RESULTS

The shielding evaluation of the GBC-32 cask is done by calculating n-g dose rates in axial and radial direction of the cask, to demonstrate compliance with 10CFR71 regulatory limits on dose rates during normal and accidental cask transport. These limits are 2 mSv/h (200 mrem/h) at the cask surface and 0.1 mSv/h (10 mrem/h) at 2 m from the cask. The same dose rates under hypothetical accidental scenario have higher dose limits of 10 mSv/h (1000 mrem/h) at 1 m from the cask surface. The accidental cask model has impact limiters and neutron resin shield removed.

The shielding analysis was performed by using SCALE6.1.3/MAVRIC sequence for optimized 3D MC calculations of cask's radiation field. The obtained results show compliance with 10CFR71 regulatory limits in all cases. The cylindrical mesh tally was used to capture n-g global flux convergence and derived n-g dose rates (in rem/h) around the cask exterior. Additionally, point detectors were placed in cask midplane, extending radially from cask's surface to 2 m distance using steps of 50 cm.

A. MAVRIC RESULTS FOR ANALOG MC AND GENERIC CASK SOURCE

Figures 4 to 6 show analog MC results of neutron dose rates - neutrons penetrate more easily through 35 cm thick SS304 shield compared to gamma-rays, but statistical noise is still unacceptably high in obtained dose axial profiles (Figure 5). The neutron dose maximum is in upper and lower cask region, reaching values above the 0.1 rem/h. The Monaco MC module was used with 500 batches and 2000 neutrons per batch using broad shielding library "v7-27n19g". For photon case, with noticeable slow MC convergence, these values were higher, i.e. 5000 batches and 10000 per batch. The total CPU time was 650 min for neutrons and 716 min for photons. Compared to neutrons, photons are unable to penetrate outer steel body of the cask, leaving the exterior without the results (Figure 6).

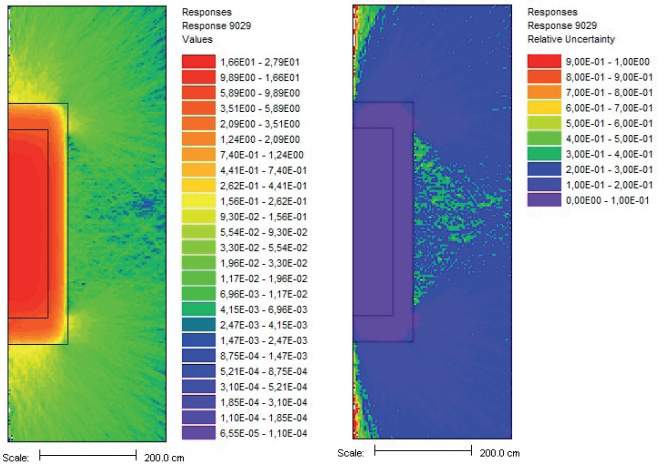

Fig. 4. Neutron dose rates (rem/hr) with errors (analog MC)

Mario Matijević, Matej Pekeč, Hybrid Shielding Calculations of GBC32 Cask, Journal of Energy, vol. 75 Number 1 (2026), 3–8
https://doi.org/10.37798/2026751724

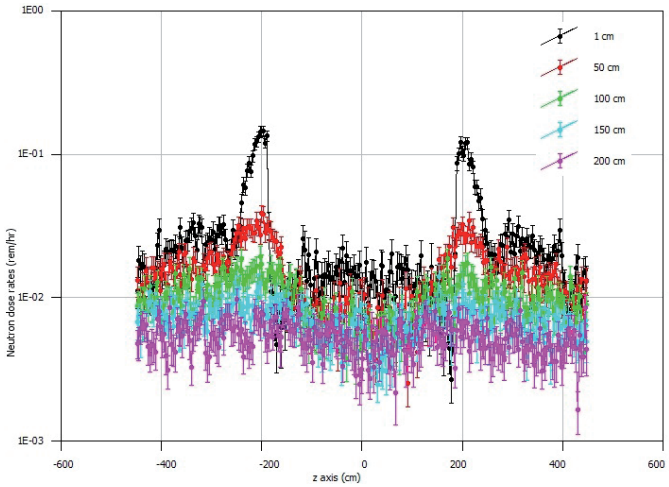

Fig. 5. Neutron dose (rem/h) axial profiles (analog MC)

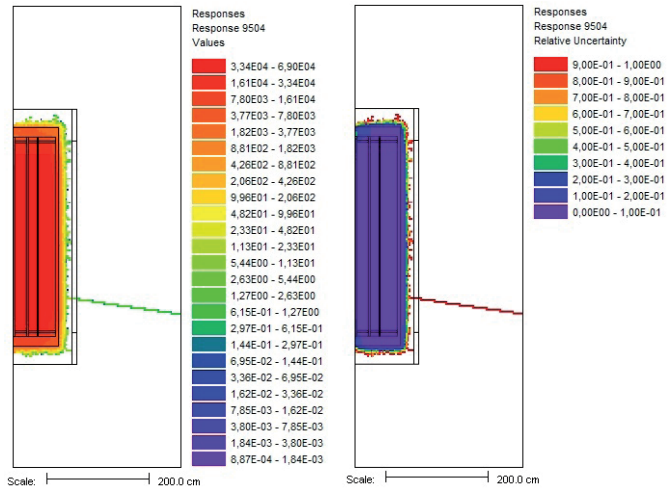

Fig. 6. Photon dose rates (rem/hr) with errors (analog MC)

B. MAVRIC Results for FW-CADIS and Generic Cask Source

The same n-g shielding calculations were repeated by using FW-CADIS methodology of MAVRIC shielding sequence. Total CPU time was 404 min for neutron case and 921 min for photon case. The number of particles simulated was the same as in analog cases. The FW-CADIS variance reduction technique was used to improve the overall transport of neutrons and photons. Figures 7 and 8 show significant improvement in MC statistics and neutron dose distribution, which can also be seen in axial and radial curve profiles for different distances from the cask. As expected, the neutron streaming is pronounced near upper and lower cask region, reaching maximum about 0.01 rem/h at the cask surface, well below regulatory limit of 0.2 rem/h. For a 2 m dose limit (0.01 rem/h), Figure 7 also depicts dose rates above that limit, indicating compliance with regulations.

Figures 9 and 10 show optimized distribution of gamma doses for FW-CADIS and generic source, with an axial and radial dose profiles; the dose difference between upper and lower cask plates are due to axial burnup profile function which was used for source particle biasing. The dose limits by 10CFRPart71 are again met, even though photon simulation exhibits a slow MC convergence.

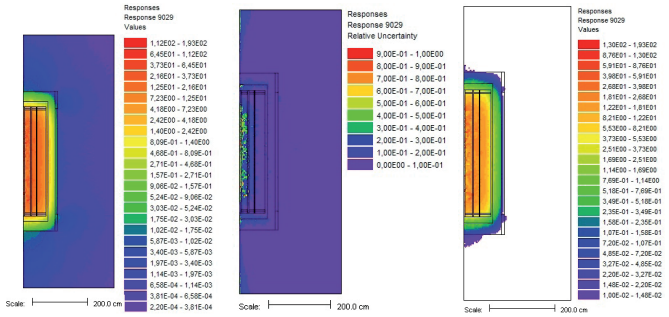

Fig. 7. Neutron dose rates (rem/h) with errors and values above the 2 m regulatory limit

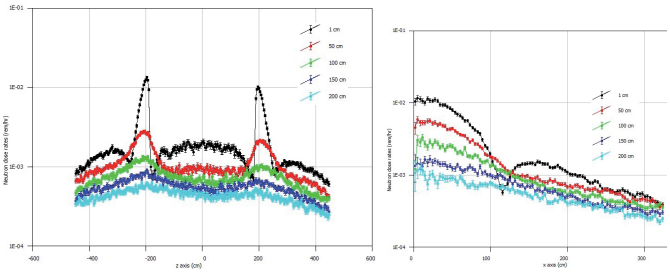

Fig. 8. Neutron dose rates (rem/h) axial and radial profiles (generic source)

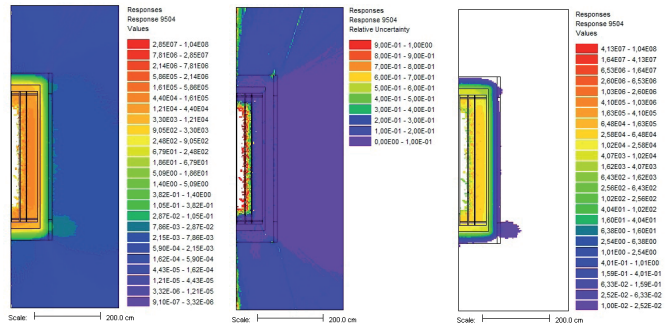

Fig.9. Gamma dose rates (rem/hr) with errors and values above the 2 m regulatory limit

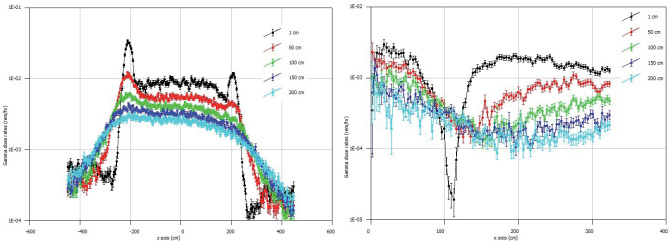

Fig. 10. Gamma dose rates (rem/h) axial and radial profiles (generic source)

C. MAVRIC Results for FW-CADIS and Realistic Cask Source

This set of n-g calculations is addressing a more realistic cask source with a three fuel regions or zones, where each zone is described with specific (averaged) values of fuel enrichment, burnup and cooling time. The zonal values were taken as representative, real-life cases. These MC calculations are more complex, since biased source sampling is performed using 3-zonal particle spectra for active fuel, hardware activation spectrum for 3 axial regions per FA and axial burnup profile for spatial biasing, making distinction between neutrons and gammas. The MC and SN parameters remain the same as in previous calculations.

Mario Matijević, Matej Pekeč, Hybrid Shielding Calculations of GBC32 Cask, Journal of Energy, vol. 75 Number 1 (2026), 3–8
https://doi.org/10.37798/2026751724

Figure 11 shows results of neutron dose rates (rem/h) calculated by FW-CADIS for three-zone fuel pattern, clearly influencing dose profiles in axial direction of the cask, shown in Figure 12. Additionally, the values above the dose regulatory limit for 2 m distance (0.01 rem/h) from the cask are also shown in Figure 11, clearly indicating compliance with the limit. As expected, the dose maximum corresponds to a region with a least attenuating material, which are typically ventilation openings. The difference in upper and lower dose maximum are due to inclusion of axial burnup profile used as a spatial sampling function.

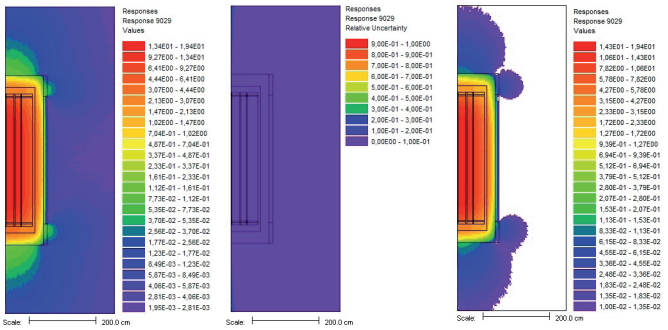

Fig. 11. Neutron dose rates (rem/hr) with errors and values above the 2 m regulatory limit

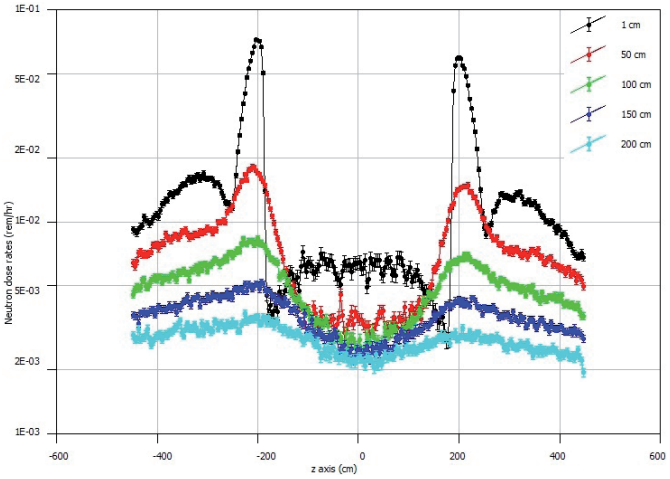

Fig. 12. Neutron dose rates (rem/h) axial profiles (realistic source)

Figure 13 shows results of gamma dose rates (rem/h) calculated by FW-CADIS for three-zone fuel pattern, again influencing dose profiles in axial direction of the cask, shown in Figure 14. The values above the dose regulatory limit for 2 m distance (0.01 rem/h) from the cask are again shown in Figure 13, clearly indicating compliance with the regulatory limit. The dose rates maximum again corresponds to upper and lower cask regions, while the difference in upper and lower dose maxima are due to inclusion of axial burnup profile.

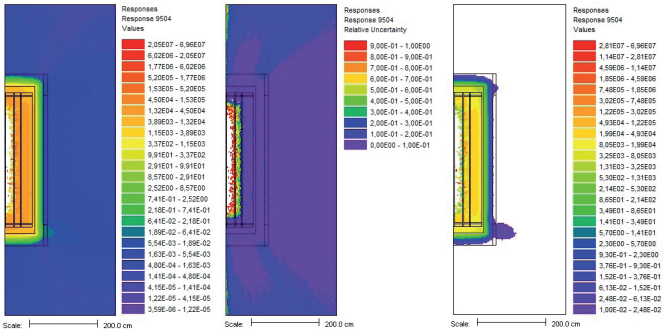

Fig. 13. Gamma dose rates (rem/hr) with errors and values above the 2 m regulatory limit

One should also notice an excellent MC dose rate convergence by FW-CADIS method, in both neutron and gamma case, covering almost uniformly the simulation model with particles. The global unit has dimensions of 6.5x6.5x9 m, where cask dimensions are cca 5 m in height and 2.5 m in diameter. The CPU time for neutron dose case was 3.6 hr (SN) and 30 hr (MC), and for gamma dose case was 1.0 hr (SN) and 29 hr (MC).

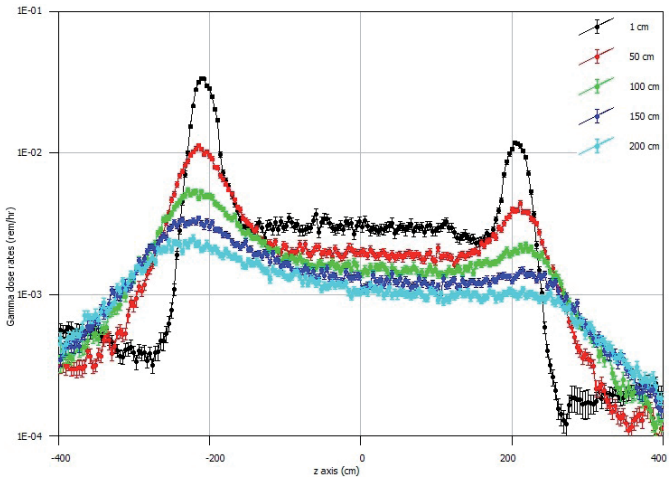

Fig. 14. Gamma dose rates (rem/h) axial profiles (realistic source)

Summary of neutron and gamma dose rates on point detectors (PDs) with variable radial distance in the cask midplane are presented in Table 3 for all simulated n-g cases. The abbreviated names for cases are the following: "generic" is for a uniform (one fuel zone) source, "realistic" is for a nonuniform (three fuel zones) source, "analog" is for MC without VR parameters, and "FW-CADIS" is for deterministically obtained VR parameters. The FAs in outer region (or zone) of the cask basket are basically driving the received dose rates since interior sources are being self-shielded.

TABLE III.
SUMMARY OF DOSE RATES (REM/HR) IN CASK MIDPLANE

PD	Neutrons (generic, analog)	Neutrons (generic, FW-CADIS)	Neutrons (realistic, FW-CADIS)	Photons (generic, analog)	Photons (generic, FW-CADIS)	Photons (realistic, FW-CADIS)
1.	1.2e-2±35%	1.0e-3±25%	8.0e-3±20%	9.6e-3±91%	9.5e-3±8.5%	6.4e-3±6.9%
2.	8.4e-3±3.8%	6.6e-4±2.8%	3.9e-3±1.8%	1.9e-3±49%	6.5e-3±1.8%	3.4e-3±1.7%
3.	6.4e-3±2.3%	5.3e-4±1.7%	3.0e-3±0.7%	6.5e-3±84%	4.6e-3±1.3%	2.3e-3±1.1%
4.	5.6e-3±1.9%	4.6e-4±1.9%	2.6e-3±0.5%	8.2e-3±91%	3.5e-3±1.0%	1.8e-3±1.0%
5.	4.8e-3±1.4%	3.8e-3±1.1%	2.3e-3±0.5%	8.5e-3±93%	2.8e-3±0.9%	1.4e-3±0.8%

D. MAVRIC Results for Accidental Case

This last set of calculations presents shielding evaluation of the accidental cask condition, where neutron dose rates clearly meet the regulatory limit of 10 mSv (1 rem/h) at 1 m from the cask surface. The MC simulation model is the same as in the previous section (realistic source using FW-CADIS), but with the impact limiter (wood) and neutron shield (resin) removed from the cask body exterior. It is assumed how this modification will make a marginal effect on photon transport, so only a neutron simulation was performed.

The effect of wood and resin removal is clearly seen in Figure 15, with augmented dose rates around the cask body by streaming neutrons. One can notice maximum of dose rates shifting from vent openings to the cask midplane in Figure 16. However, this is still below the regulatory limit, which can be seen in Figure 15 using the threshold operator, setting the minimum dose values to 1 rem/h.

Mario Matijević, Matej Pekeč, Hybrid Shielding Calculations of GBC32 Cask, Journal of Energy, vol. 75 Number 1 (2026), 3–8
https://doi.org/10.37798/2026751724

The dose rates profiles along the cask axial dimension, for different distances from the cask surface, are shown in Figure 16. The neutron dose rates peak at the cask midplane with surface, 1m and 2 m neutron dose values corresponding to 0.2 rem/h, 0.09 rem/h and 0.04 rem/h.

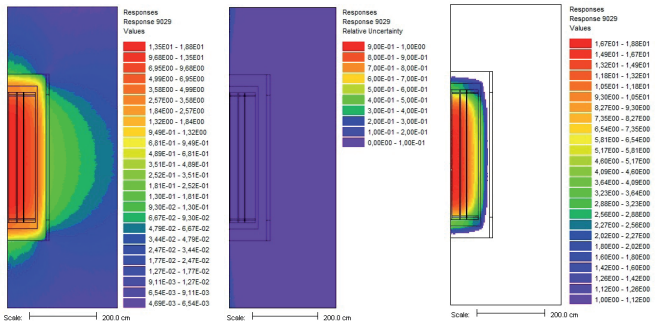

Fig. 15. Neutron dose rates (rem/hr) with errors and values above the 1 m regulatory limit

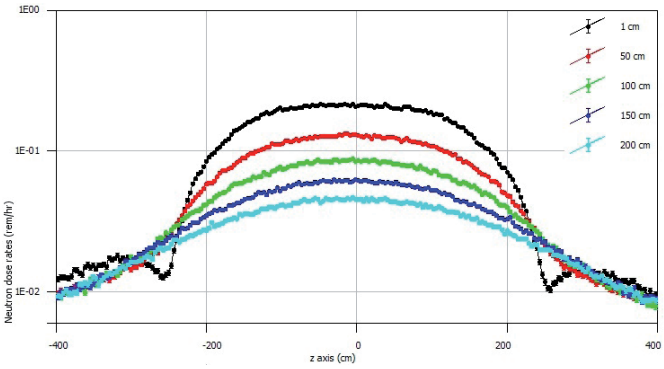

Fig. 16. Neutron dose rates (rem/h) axial profiles (accidental case)

Additional effort was put in visualisation of ratio accidental-to-normal neutron dose rates, by using MAVRIC auxiliary programs for mesh tally object formatting. The user has an option to split mesh tally object into independent families and to divide their values. Such relative ratio of neutron dose rates is shown in Figure 17 with an extra 3D plot using VisIt code [13], showing maximum jump of cca 50 in relative dose ratio at the cask surface in axial direction.

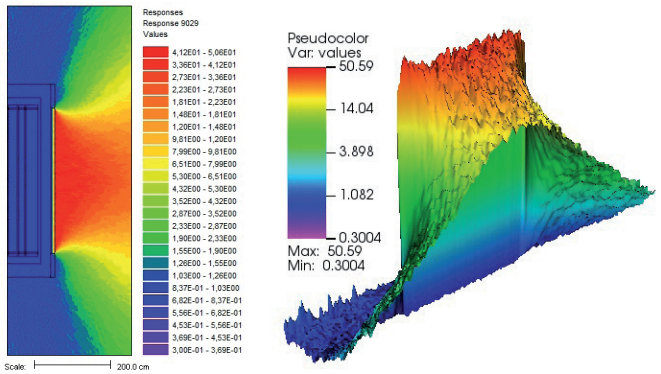

Fig. 17. Neutron dose rates relative ratio (accidental-to-normal)

Conclusion

The shielding performance of GBC-32 cask was quantified to demonstrate compliance with the dose rate limits of 10CFRPart71 for normal and accidental conditions. For that purpose, two different levels of detail were used for the source specification: a generic source (1 fuel zone) and more realistic source (3 fuel zones), using averaged values for enrichment, burnup and cooling time. An analog MC simulation was first performed, giving low quality MC results with a high statistical noise, especially for photon case. To remedy this situation, the FW-CADIS method was used to optimise neutron-gamma radiation field and dose rates around the cask, taking previously prepared source terms with ORIGEN-ARP module. The multisource problem included spent fuel neutrons and photons, photons from (n,g) reactions and photons from activated upper/lower hardware regions of spent fuel assemblies. The presented MC dosimetry results correspond to normal cask conditions, but an accidental scenario was also investigated, for which the resin neutron shield was removed from the shielding configuration. The obtained dose rate values proved to be well below regulatory limits, indicating compliance of the cask shielding design under normal and accidental conditions.

Acknowledgement

The work was carried out as part of the project HRZZ-IP-2024-05-4011 of the Croatian Science Foundation.

References

[1] "Computational Benchmark for Estimation of Reactivity Margin from Fission Products and Minor Actinides in PWR Burnup Credit", Prepared by J. C. Wagner, NUREG/CR-6747, ORNL/TM-2000/306.

[2] "Recommendations for Shielding Evaluations for Transport and Storage Packages", NUREG/CR-6802, ORNL/TM-2002/31, Prepared by B. L. Broadhead.

[3] "OrigenArp Primer: How to Perform Isotopic Depletion and Decay Calculations with SCALE/ORIGEN", prepared by S. M. Bowman, I. C. Gauld, ORNL/TM-2010/43.

[4] "SCALE: A comprehensive Modeling and Simulation Suite for Nuclear Safety and Design", ORNL/TM-2005/39, Version 6.1, June 2011. Available from Radiation Safety Information Computational Center at Oak Ridge National Laboratory as CCC-785.

[5] M. Matijević, M. Pekeč, "Characterization of the GBC-32 Fuel Assembly Source Terms", Vol. 71, No. 4 (2022), Journal of Eenergy - ENERGIJA (04/2022), https://doi.org/10.37798/2022714467

[6] B.W. Kernighan, D.M. Ritchie, The C Programming Language, 2nd Edition, Prentice Hall, 1988.

[7] J. C.Wagner and A. Haghighat, "Automated variance reduction of Monte Carlo shielding calculations using the discrete ordinates adjoint function," Nuclear Science and Engineering, Vol. 128, no. 2, pp. 186–208, 1998.

[8] J. C. Wagner, E. D. Blakeman, and D. E. Peplow, "Forward weighted CADIS method for global variance reduction," Transactions of the American Nuclear Society, vol. 97, pp. 630–633, 2007.

[9] T. M. Evans, A.S. Stafford, R.N. Slaybaugh, K.T. Clarno, "Denovo: A New Three-Dimensional Parallel Discrete Ordinates Code in SCALE," Nuclear Technology, 171:2, 171-200, DOI: 10.13182/NT171-171, 2010.

[10] G. I. Bell and S. Glasstone, "Nuclear Reactor Theory," Van Nostrand Reinhold Company, Litton Educational Publishing, 1970.

[11] E. E. Lewis, W. F. Jr. Miller, "Computational Methods of Neutron Transport", American Nuclear Society, Illinois, 1993.

[12] M. B. Chadwick, P. Obložinsky, M. Herman et al., "ENDF/B-VII.0: next generation evaluated nuclear data library for nuclear science and technology," Nuclear Data Sheets, Vol. 107, no. 12, pp. 2931–3060, 2006.

[13] VisIt: An End-User Tool for Visualizing and Analyzing Very Large Data, VisIt User's Manual, Version 1.5, UCRL-SM-220449, Lawrence Livermore National Laboratory, Weapons and Complex Integration, 2005.